Dhavale *et al.*
Bulletin of the National Research Centre (2023) 47:18
https://doi.org/10.1186/s42269-023-00990-6

Bulletin of the National Research Centre

RESEARCH

Open Access

Sialylation of chitosan to mitigate Aβ toxicity

Dhruva Dhavale[1], Hy K. Lai[3], Paityn Warwick[2] and James E. Henry[3*]

Abstract

Background Amyloid beta peptide (Aβ) is the main component of plaques and is known to play a role in the development of Alzheimer's disease (AD). As a result, structures that can trap Aβ or disrupt the interaction between Aβ and cells have been researched as a way to lessen the pathological effects of Aβ. Particularly, sialylated compounds that exhibit clustering effects could be advantageous.

Results Through the use of 1-ethyl-3-(3-dimethylaminopropyl)carbodiimide chemistry, sialic acid (N-acetylneuraminic acid) was used to decorate a chitosan backbone. The compounds were characterized using Fourier-transform infrared spectroscopy (FTIR) and colorimetric assays. Using the model neuroblastoma cell line SH-SY5Y, the ability of these compounds to lessen the toxicity of Aβ was examined in vitro. Successful in vitro mitigation of Aβ toxicity was found to be critically dependent on the degree of sialylation. In particular, a balance between the degree of sialylation and molecular flexibility was determined to be the criteria as it allows for natural clustering. Additionally, chitosan alone demonstrated low levels of cellular toxicity with moderate levels of toxicity mitigation (comparable to low degrees of labelling).

Conclusions Compounds were successfully produced, and they varied in their effectiveness in reducing Aβ's toxicity to cells in culture. The effect of molecular flexibility and clustering on toxicity mitigation is explained in this work. This shows the potential of polymeric sugars for the creation of AD treatments.

Keywords Alzheimer's disease, Amyloid, Sialic acid, Toxicity, Aggregation

Background

More than 6 million Americans will be affected by Alzheimer's disease (AD) in 2022, making it the leading cause of neurodegeneration in the USA. The majority of the estimated $321 billion cost was attributable to continued care for patients who were no longer capable of caring for themselves (Alzheimer's Association 2022). Although there are numerous hallmarks of Alzheimer's disease (such as neurofibrillary tangles and amyloid plaques), we will focus on fibrils, of which Aβ is the primary protein component. We chose this target because it is widely believed that Aβ is the principal agent responsible for AD-related neurodegeneration.

A number of researchers, including ourselves, have hypothesized that Aβ binds to cell membranes via interaction with gangliosides or glycoproteins containing sialic acid on the cell surface (Ariga et al. 2001; Kakio et al. 2003; Wakabayashi et al. 2005; Patel et al. 2007, 2006; Murray et al. 2016; Rawal and Zhao 2021; Matsuzaki 2020; Shin et al. 2019; Fantini et al. 2020). Numerous studies (Ariga et al. 2001; Kakio et al. 2003; Patel et al. 2007, 2006; Murray et al. 2016; Sgambati et al. 2022; Choo-Smith and Surewicz 1997; Chaudhary et al. 2019) have demonstrated that the binding affinity of Aβ to the membrane is greater when multiple sialic acids are present, either due to the clustering of gangliosides or the degree of sialylation of gangliosides. Previously synthesized membrane-mimetic multivalent sialic acid

*Correspondence:
James E. Henry
jhenry13@lamar.edu
[1] Cain Department of Chemical Engineering, Louisiana State University, 110 Chemical Engineering, South Stadium Road, Baton Rouge, LA 70803, USA
[2] Department of Biology, Lamar University, 101 Hayes Building, Beaumont, TX 77710, USA
[3] Dan F. Smith Department of Chemical and Biomolecular Engineering, Lamar University, 101 Lucas Engineering, Beaumont, TX 77710, USA

polymers have been found to reduce toxicity (Patel et al. 2007, 2006; Evangelisti et al. 2016; Rudajev and Novotny 2020; Gupta et al. 2019; Wu et al. 2021), induce Aβ aggregation, and promote plaque formation (Sgambati et al. 2022; Zaman et al. 2018; Lünemann et al. 2021). These materials also bind to Aβ with high affinity (association binding constants on the order of 10^7 to 10^8 M^{-1}, compared to 10^6 to 10^7 M^{-1} for sialic acid-containing membranes to Aβ) (Patel et al. 2007, 2006; Sgambati et al. 2022; Cowan et al. 2009, U 2009). Core polymer toxicity was a major issue. This work addresses this deficiency by employing chitosan as the core backbone polymer, as chitosan is FDA-approved for implantation(Wang et al. 2020a, 2020b; Negm et al. 2020; Azmana et al. 2021).

Methods

Materials

The beta peptide was sourced from Anaspec Inc. (San Jose, CA). ATCC was used to source the human neuroblastoma SH-SY5Y cells (Manassas, VA). All material necessary for culturing the cells were obtained from Invitrogen (Grand Island, NY). Chitosan powder with mean molecular weight of 15,000 was sourced from Polysciences Inc. (Warrington, PA). Pierce Biotechnology (Rockford, IL) supplied 1-Ethyl-3-(3-dimethylaminopropyl)carbodiimide (EDC) and Sulfo-NHS. Separation units were sourced from Millipore (Billerica, MA). Invitrogen was utilized to purchase the eBioscience Annexin V Apoptosis Detection Kit (Waltham, MA). All additional chemicals and materials not mentioned previously were sourced from Sigma-Aldrich (St. Louis, MO).

Peptide preparation

The Aβ fibrils were generated using techniques previously developed and published as standard techniques from the production of toxic fibril species (Patel et al. 2006; Rymer and Good 2001). Before making the aggregated Aβ peptide, the lyophilized powder of Aβ peptide was dissolved in 1,1,1,3,3,3-Hexafluoro-2-propanol (HFIP). The HFIP solution was then dried overnight. The resulting dry peptides film of Aβ (1–40) was dissolved in DMSO at concentration of 10 mg/ml and incubated for 1 h at 25 °C to generate a stock solution for future fibril formation. After incubation, stock solutions of Aβ were diluted to their final concentrations in cell culture medium and aggregated at 25 °C for 24 h under rotational mixing before addition to the cultures. Literature indicates that the described method produces fibrils that are consistently toxic in vitro at the utilized concentrations (Patel et al. 2006; Rymer and Good 2001). Aβ (1–40) peptide was used to maintain consistency with previous works to allow for direct comparison. While we recognize that Aβ (1–42) is inherently more toxic, Aβ(1–40) peptide is the most abundant Aβ form in the human brain, with Aβ(1–42) showing a significant increase with certain forms of AD (Schmidt et al. 2009).

Cell culture

SH-SY5Y cells were grown in Minimum Essential Media (MEM) containing 10% (vol/vol) fetal bovine serum, 2.2 mg/ml $NaHCO_3$, 100U/ml penicillin, 100 g/ml streptomycin, and 2.5 g/ml amphotericin-B. (fungizone). Prior to their use in toxicity experiments, SH-SY5Y cells were differentiated with 20 ng/ml NGFβ for 5–7 days in 96-well plates. All cells used in experiments were less than 10 passages old to ensure consistency in cellular response.

Sialic labeled chitosan: synthesis and purification

Using EDC chemistry, sialic acid was conjugated with chitosan according to the manufacturer-recommended protocol, with minor modifications. Chitosan was dissolved in PBS to a final concentration of 8 mg/ml. Utilizing information from the supplier, the number of available primary amines on the chitosan backbone was determined from the degree of glycosylation (approximately 84%). This value was then used to determine the concentrations of sialic acid and EDC to be used during conjugation. To determine the effect of varying labeling densities, the ratio of sialic acid to amines was varied. A sialic acid conjugation solutions of varying concentrations was created using activation buffer (pH 6 solution of MES and 0.5 M NaCl). 1.1 mg of Sulfo-NHS and 0.3626 mM of EDC were added to this activated buffer solution. The pH was maintained between 5.0 and 6.0 by using a phosphate buffer of 0.1 M. (at pH 7.2). The reaction mixture was continuously rotated for 15 min at room temperature. The unreacted EDC was then rendered inactive by adding 1.4 l of 2-mercaptoethanol. The reaction mixture was stirred for 2 min before 1 ml of chitosan solution was added, the pH was adjusted to 7.0 with phosphate buffer, and the mixture was left to react overnight. The reaction mixture was examined for precipitation after 24 h. Before purification, the resultant precipitate was dissolved by adding 10% (vol/vol) acetic acid solution drop by drop.

To remove unreacted sialic acid and EDC from the reaction volume, a 10,000 NMWL cutoff ultra-centrifugal filter unit was utilized for ultrafiltration. Each time, six DI water washes were performed to remove any free (unbound) sialic acid still remaining (Patel et al. 2006). The resulting solution was stored in darkness at − 4 °C.

Verification and quantification of extent of sialic acid conjugation

Using an Fourier-transform infrared spectroscopy (FTIR) outfitted with attenuated total reflection (ATR) capability, the presence of sialic acid on chitosan was determined. Compound samples of sialic acid-chitosan conjugates were lyophilized for FTIR analysis. All samples were freeze-dried and desiccated prior to analysis. This includes naïve chitosan that was scan to develop an unconjugated baseline.

Sialic acid attachment was determined using (Warren 1963; Cheeseman et al. 2021) method. The free sialic acid was subjected to periodic oxidation in this method, resulting in the formation of formyl pyruvic acid. This resulting compound reacts with two molecules of thiobarbituric acid to generate a red solution. The resulting solution was spectroscopically analyzed at 549 nm. The Warren test employs the subsequent solutions:

(a) 0.2M Sodium (meta) periodate in 9M phosphoric acid (prepared fresh each time)
(b) 10% (w/v) Sodium arsenite in a solution of 0.5M sodium sulphate-0.1M H_2SO_4
(c) 0.6% (w/v) Thiobarbituric acid in a solution of 0.5M sodium sulphate

The procedure to determine the extent of sialic acid labeling is as follows (Warren 1963):

(a) A sample containing 0.3 mM of bound sialic acid (assuming 100% attachment efficiency) was treated at 80 °C for 1 h with 0.1N HCl.
(b) 0.2 ml of the resulting sample is treating with 0.1 ml of periodate solution (a) and incubated at room temperature for 20 min.
(c) The solution from step 2 is treated with 1 ml of arsenite solution (b) and agitated until the solutions turned clear.
(d) The solution was then treated with 3 ml of thiobarbituric acid solution (c). The solutions were agitated and incubated in a boiling water bath for 15 min. Any presence of a white color indicates failure of step 3 and requires the sample to be discarded.
(e) The solution was incubated in a water bath for 5 min for color development.
(f) The solution was treated with 4.3 ml of Cyclohexanone and agitated.
(g) The solution was then centrifuged at 1500 g and 25 °C for 7 min to phase separate the water and cyclohexane phases. The color should be primarily collected in the organic phase.
(h) The resulting cyclohexane phase (the top layer) was collected and the absorbance was measured at 549 nm.

This procedure was also utilized to develop a standard curve for free sialic acid in solution and on chitosan to verify no interference in the underlying assay.

MTT toxicity assay

SH-SY5Y cells were seeded at a density of 2×10^4 cells per well in 96-well plates, and NGF was used to induce differentiation for 5.7 days. After incubation, the media was replaced by fresh media containing the either Aβ, chitosan with varying degrees or sialylation, or both. Using methods described in earlier sections, a 50uM concentration of Aβ peptide was prepared. In each experiment, Aβ was added to the cells approximately 30 min before chitosan or conjugated compound was added. On a 96-well plate, a gradient of chitosan and conjugated compound from 30 to 1 M was applied. Following the addition of Aβ, chitosan, and chitosan conjugated with sialic acid for 24 h, the viability of cells was determined using the MTT assay. The media in the wells were replaced with 100ul of media devoid of phenol red. 10ul of a freshly prepared 5 mg/ml MTT solution was added to each well in a culture medium without phenol red. After two hours of incubation, the cells were examined for the presence of purple crystals and the medium was replaced with 200ul of DMSO and incubated with mixing for 20 min. The resulting samples were measure optically at 570 nm and 690 nm to determine the concentration of formalin. The resulting viabilities were divided by the sample control viability (no adulterants in the media to normalize for comparison.

Apoptosis assay

SH-SY5Y viability was determined using Annexin V PE and 7-AAD staining. Annexin V in a fluorescently labeled phospholipid binding protein that indicates a cell marked for phagocytosis (undergoing apoptosis). 7-AAD is a nucleic acid binding protein that is excluded by living cells. Cells that exhibit response to the dyes can be categorized according to Table 1.

Table 1 Cell status mapping for apoptosis assay

Cell phase	Annexin V PE status	7-AAD status
Alive	Negative	Negative
Early apoptotic	Positive	Negative
Late apoptotic	Positive	Positive
Necrotic	Negative	Positive

SH-SY5Y cells were plated in 96-well plates to a concentration 2×10^4 cells per well. After 4 days, the media was removed and replaced with medium containing 50uM Aβ. 30 min later, 30uM of the compound to be tested (chitosan, fourfold, or tenfold SA conjugated chitosan) was added and the system was incubated for 24 h. Following incubation, the cells were prepared for flow cytometry by detaching cells from the wells by using 150µL of dissociation buffer at room temperature for 10 min. 5µL of Annexin V PE conjugate was added to each well and left to incubate at 25 °C for 15 min in the dark after brief shaking. The liquid was decanted after centrifugation (1400 rpm for 5 min), after with 5µL of 7-AAD solution was added to each well and left to incubate for an additional 20 min. Immediately after, cell fluorescence was measured with the FCMS (BD FACSMelody, Becton Dickinson, Bedford, MA). Cells were analyzed using a blue laser pathway (488 nm) with fluorescence measured using 586/42 nm and 700/54 nm filters to detect Annexin V PE and 7-AAD, respectively. Flow rates were adjusted to maintain an event rate of 500 events/second with a total event threshold of 10,000 events. The low event rate was maintained to prevent signal overlap between samples and to maximize the accuracy of the results. Gating was done to obtain percentages of the total cell population that were present in each of the four phases described in Fig. 1.

The apoptosis assay used relies on the binding of two dyes. The first, Annexin V PE relies on the interaction of Annexin V, an intracellular protein that binds to phosphatidylserine. During apoptosis, cells begin transporting phosphatidylserine from the intracellular leaflet of the plasma membrane to the external leaflet. This allows for external labelling of the cell by Annexin V, thus attaching the fluorescent PE to the cell surface of apoptotic cells in much higher concentrations than that of healthy cells.

Second, 7-AAD is a fluorescent compound with a strong binding affinity to DNA. However, 7-AAD does not cross the cellular membrane or nuclear envelop readily. As such, the cell must have undergone severe perforation of both membranes for 7-AAD to bind. This indicates either late-apoptosis or necrosis.

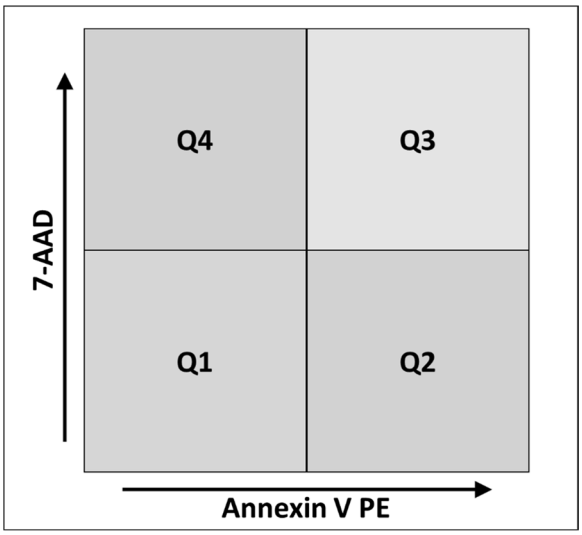

Fig. 1 Gating layout of FCMS apoptosis assay. The cells fall into one of four categories from the apoptosis assay. These categories are: Alive (Q1 – low 7-AAD and low Annexin V PE), Early apoptotic (Q2 – low 7-AAD and high Annexin V PE), Late apoptotic (Q3 – high 7-AAD and high Annexin V PE), and Necrotic (Q4 – high 7-AAD and low Annexin V PE)

Results

Validating SA conjugation

Figure 2a–c show the FTIR for Compound B (NH_2/SA = 1), Compound F (NH_2/SA = 4), Compound G (NH2/SA = 10) respectively (dashed line). The FTIR spectrum of chitosan (solid line) is overlayed to allow for better elucidation of spectral differences.

In the region between 3000 and 3500 cm^{-1}, the FTIR spectrum of pure chitosan reveals two weak peaks that are indicative of the presence of primary amines. These peaks are missing in the spectra of the compounds, thus indicating complexation of the primary amine. To further support this assertion, a broad band stretch for amide –NH frequency is also demonstrated. In the compound spectra, a strong peak at 1650 cm^{-1} indicated the presence of an amide bond. The loss of primary amines and formation of amide bonds confirmed that SA and chitosan formed a compound. We also see the loss of the C=O of carboxylic acid between 1700 and 1725 cm^{-1} in the compound spectra. This indicates little to no free sialic acid in the sample contributing to the spectra. Finally, the compound shows alcohol peaks at 1030 cm^{-1} and 1380 cm^{-1}. These peaks are expected with the presence of conjugated sialic acid, with the abundance of OH groups.

The spectra for other concentrations (compounds A, C, D, and E) are not shown, as they look similar and provide no additional complexation information. However, they were verified for attachment of sialic acid.

Quantification of sialic acid conjugation

To generate a standard curve, pure sialic acid was subjected to the Warren assay. As shown in Fig. 3, the Warren assay yields extremely precise and reproducible results with a very small standard deviation. If the sialic acid concentration in the sample was between 0.05 mM and 0.3 mM, the assay produced accurate results with higher concentrations resulting in saturation. The

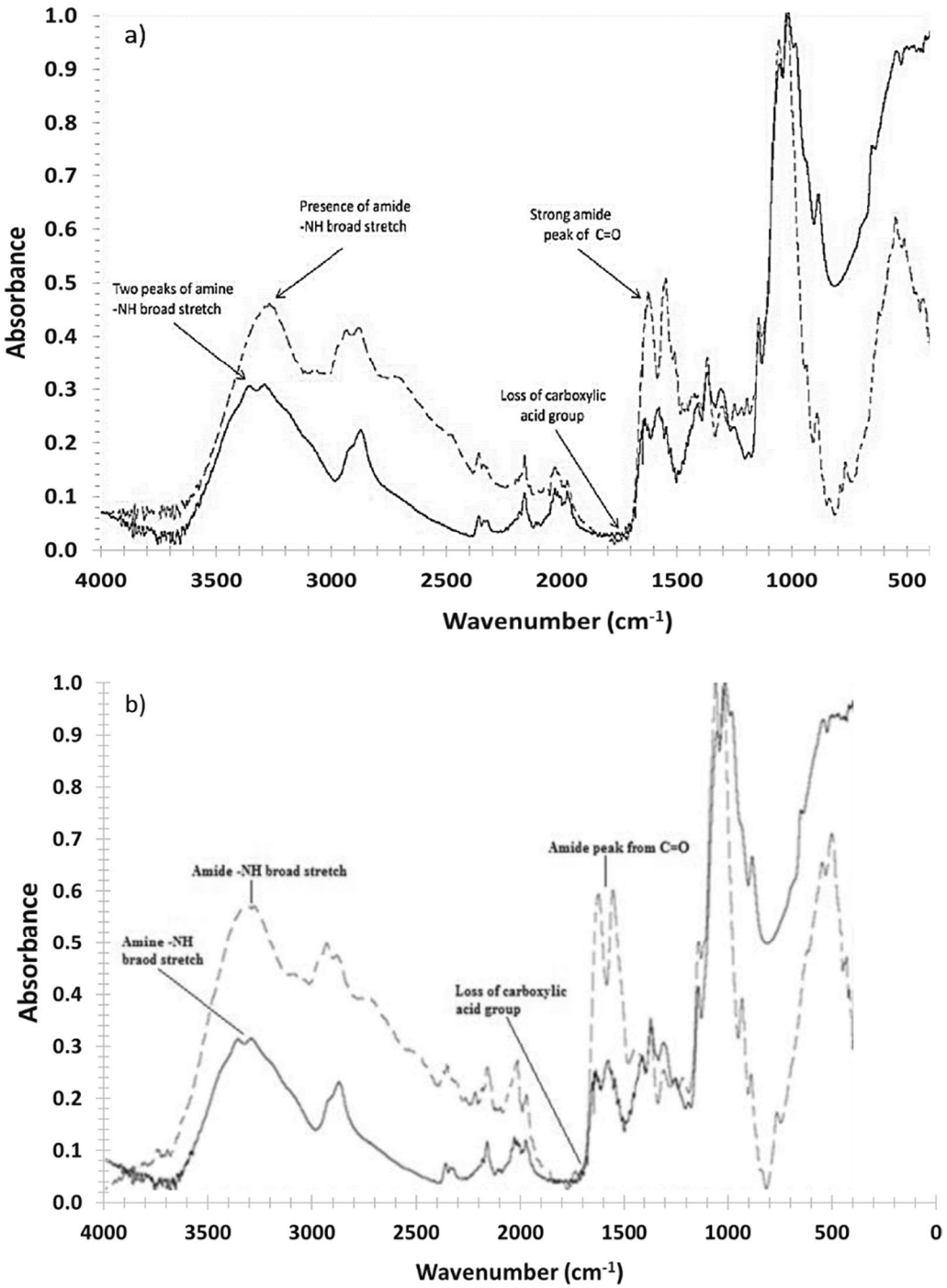

Fig. 2 FTIR spectra of chitosan compound (dashed line) and pure chitosan (solid line). **a** Compound B is produced using EDC chemistry with 1:1 ratio of sialic acid to primary amines available on the chitosan backbone; **b** Compound F is produced using EDC chemistry with 4:1 ratio of sialic acid to primary amines available on the chitosan backbone; **c** Compound G is produced using EDC chemistry with 10:1 ratio of sialic acid to primary amines available on the chitosan backbone

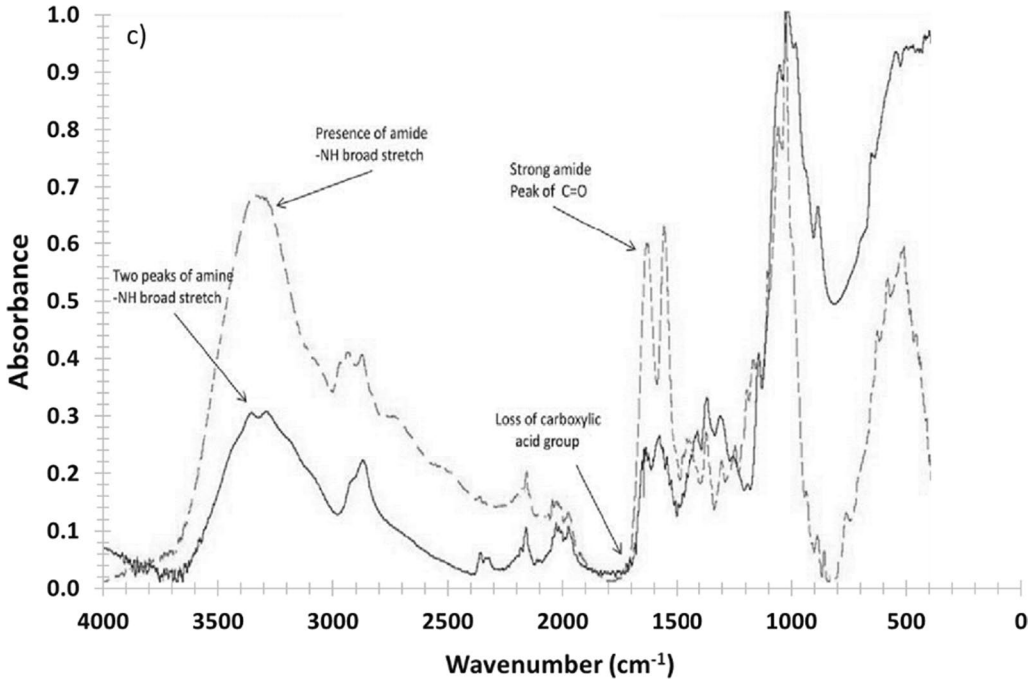

Fig. 2 continued

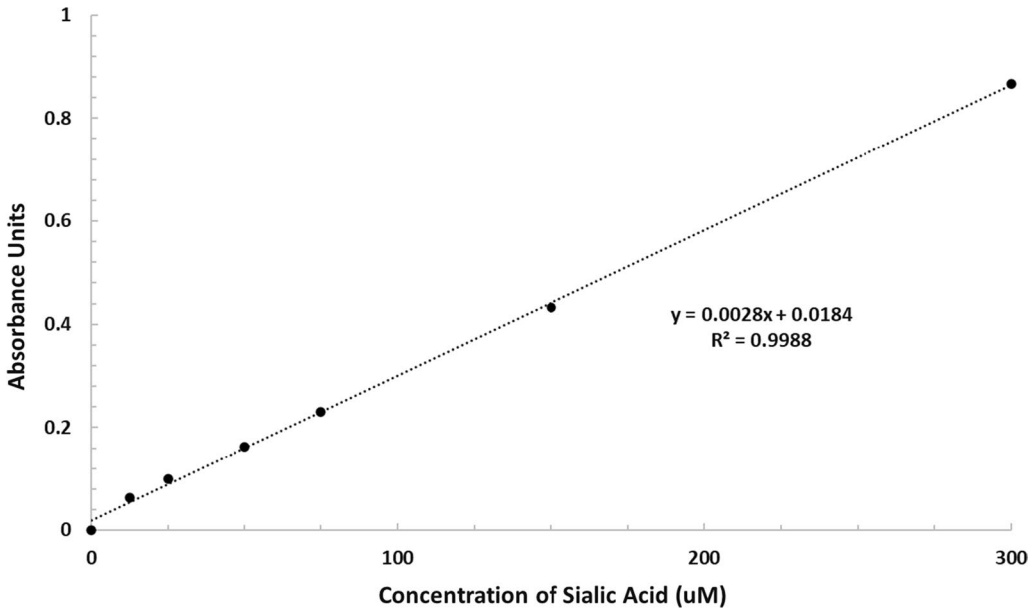

Fig. 3 Warren Assay Calibration Curve. Visible absorbance read at 549 nm with a blank of buffer without Warren reagents

Warren assay also showed no cross-reactivity with chitosan, indicating no concerns for interference with signal.

To determine the extent labeling with sialic acid, the maximum available primary amine was determined from the supplier information on degree of deacetylation of chitosan. The resulting value was the compared the sialic acid results from the Warren Assay. This was necessary as the FTIR was found to be more qualitative than quantitative, as expected. The degree of sialic acid labeling is shown in Table 2.

The conjugation chemistry follows a standard saturation curve for sialic acid labeling, as shown in Fig. 4. The

Table 2 Percent labeling of chitosan from EDC

Sample ID	[SA]:[NH2] in reaction solution	Degree of labeling (%)
A	1:4	7.8 ± 1.1
B	1:1	14.1 ± 1.9
C	1.33:1	17.6 ± 0.4
D	1.66:1	24.5 ± 0.5
E	2:1	37.3 ± 1.5
F	4:1	40.7 ± 1.4
G	10:1	48.0 ± 2.5

degree of labeling increases as the concentration of sialic acid rises until the curve begins to saturate. In addition, the data indicate that the saturation feature appears after sample C (with a ratio of amines to SA of 1). As more sialic acids link to chitosan via amine groups, it may become more difficult to accommodate further sialic acids. As the majority of SA's already present on the chitosan would prohibit free SA from interacting with the amines on chitosan, it appears doubtful that we could label chitosan to a higher degree using SA.

Efficacy of compounds to prevent toxicity

Cellular toxicity was determined via the MTT assay. The compounds were evaluated against 50uM Aβ while varying compound concentration between 1 and 30uM. Naïve compound toxicity can be seen in Fig. 5.

As can be seen from Fig. 5, an increase in labeling shows an increase in toxicity. This trend also holds for concentration, with the exception being indicated by the 10 × labeling. While there appears to be an upward trend, statistical analysis indicates that this just an artifact of the mean values, with almost no statistical relevance in the upward trend. This indicates a possible saturation effect in the 10 × sample.

After evaluating intrinsic toxicity, the compounds were evaluated for protective properties. These results are shown in Fig. 6.

As can be seen in Fig. 6, all compounds including naïve chitosan showed strong protective properties when compared to cells treated with Aβ only (0 uM concentration on the graph). The viability for all points above 0 uM sialic acid/chitosan were statistically different from the control of Aβ only using a Tukey analysis ($p < 0.05$).

Apoptosis assay

Twofold, tenfold, and naïve chitosan were tested with Aβ to determine the route of cell death. The results were compared to those for viable cells (no Aβ) and Aβ alone to compensate for cell death resulting from the other sources (cell lifting, pipetting, etc.). The results are shown in Table 3 and Fig. 7.

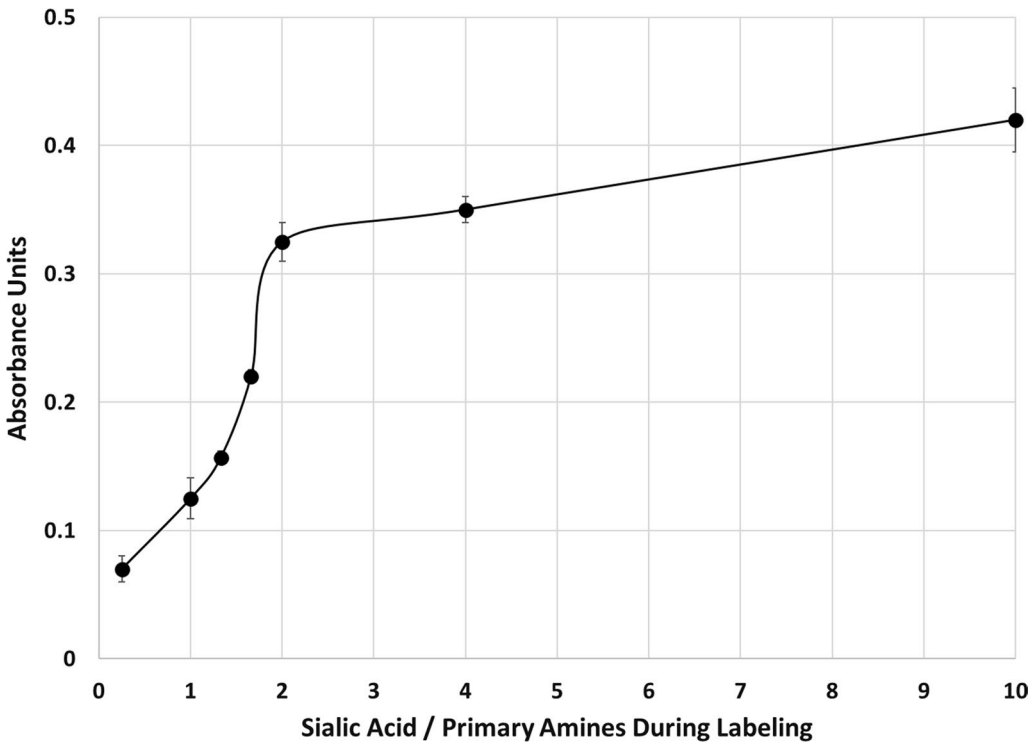

Fig. 4 Sialic acid saturation of chitosan. Letters represent the sample ID for each point with the degree of labeling shown in Table 2

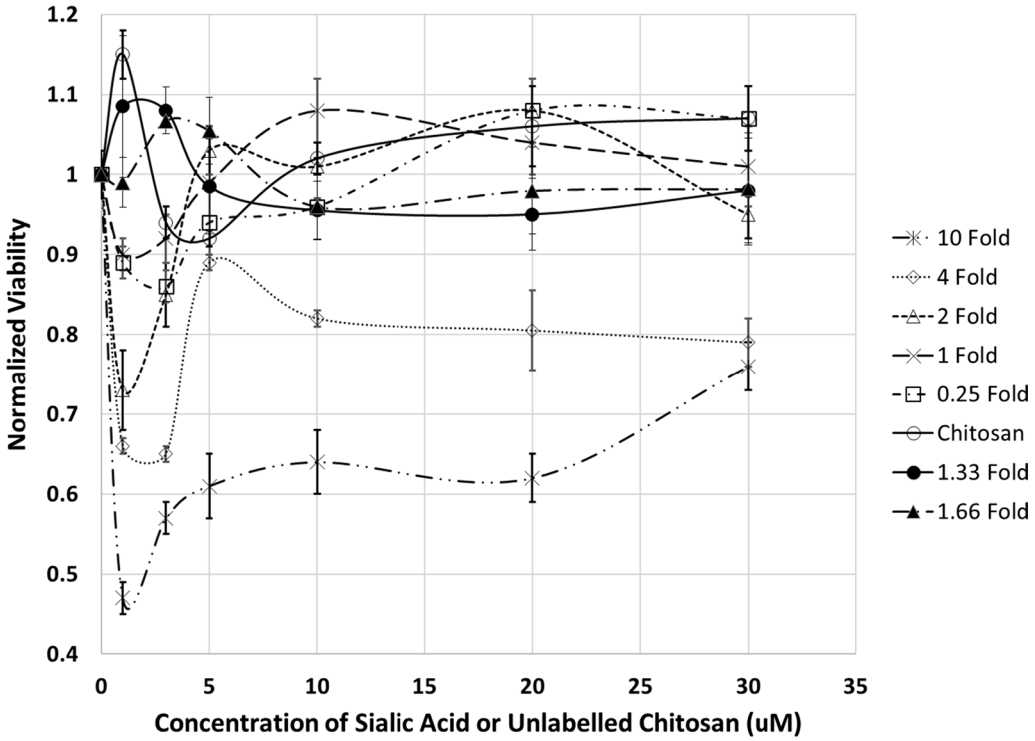

Fig. 5 Intrinsic toxicity of compounds and naïve chitosan. The lines are labeled according to the sialic acid/amine ratio in the EDC reaction mixture

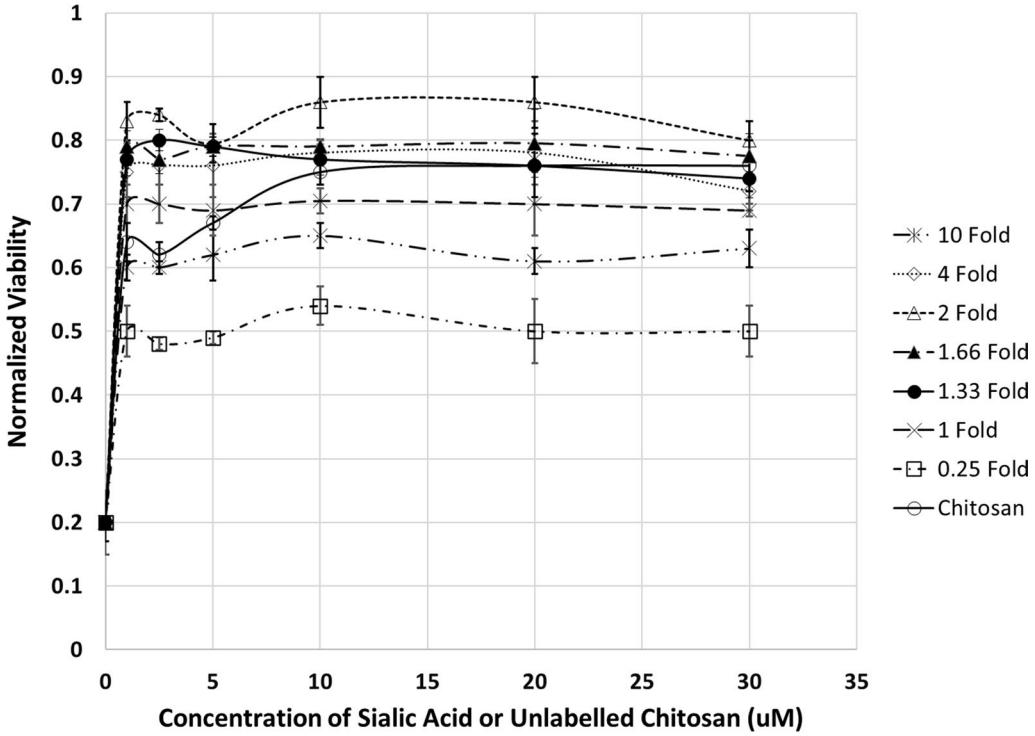

Fig. 6 Protective properties of chitosan and chitosan/SA compounds. The lines are labeled according to the sialic acid/amine ratio in the EDC reaction mixture. Aβ concentration is 50uM

Table 3 Apoptosis assay results

Sample	Alive (%)	Early apoptotic (%)	Late apoptotic (%)	Necrotic (%)
Viable	77.95	1.74	5.11	15.20
Aβ alone	33.86	14.22	36.15	15.77
Chitosan + Aβ	60.64	3.92	4.07	31.37
twofold + Aβ	73.60	6.45	6.50	13.45
tenfold + Aβ	41.66	14.53	19.6	24.21

Statistical analysis

For all compounds, Tukey analysis was performed to compare within complex set to determine the statistical variation in intrinsic toxicity. The results are found in Figs. 8(a–h).

For all low degree of labeling sample sets (naïve chitosan through complex D), there was no statistically identified intrinsic toxicity or trend of increasing toxicity with increasing concentration. However, for higher degrees of sialic acid labeling (complexes E, F, and G), there was some indication of increased toxicity, with a trend developing for complexes F and G.

Figure 9 shows a comparison of intrinsic toxicity for all complexes at each concentration of 5uM or less.

For all low degree of labeling sample sets (naïve chitosan through complex D), there was no statistically identified intrinsic toxicity or trend of increasing toxicity with increasing degree of labelling. However, for higher degrees of sialic acid labeling (complexes E, F, and G), there was some indication of increased toxicity, with a trend developing for complexes F and G, indicating much higher intrinsic toxicity for the higher degrees of labelling.

Figure 10 shows a comparison intrinsic toxicity for all complexes at each concentration 10uM or greater, with the control (no compound introduced) included for comparison.

Similar to what we saw at lower concentrations, for all low degree of labeling sample sets (naïve chitosan through complex E) at higher concentrations, there was no statistically identified intrinsic toxicity or trend of increasing toxicity with increasing degree of labelling. However, for higher degrees of sialic acid labeling (complexes F and G), there was some indication of increased toxicity, with a trend developing for complexes F and G, indicating much higher intrinsic toxicity for the higher degrees of labelling.

Similarly, Tukey analysis was performed within each complex set to determine the statistical variation in protective properties. The results are found in Fig. 11a–h

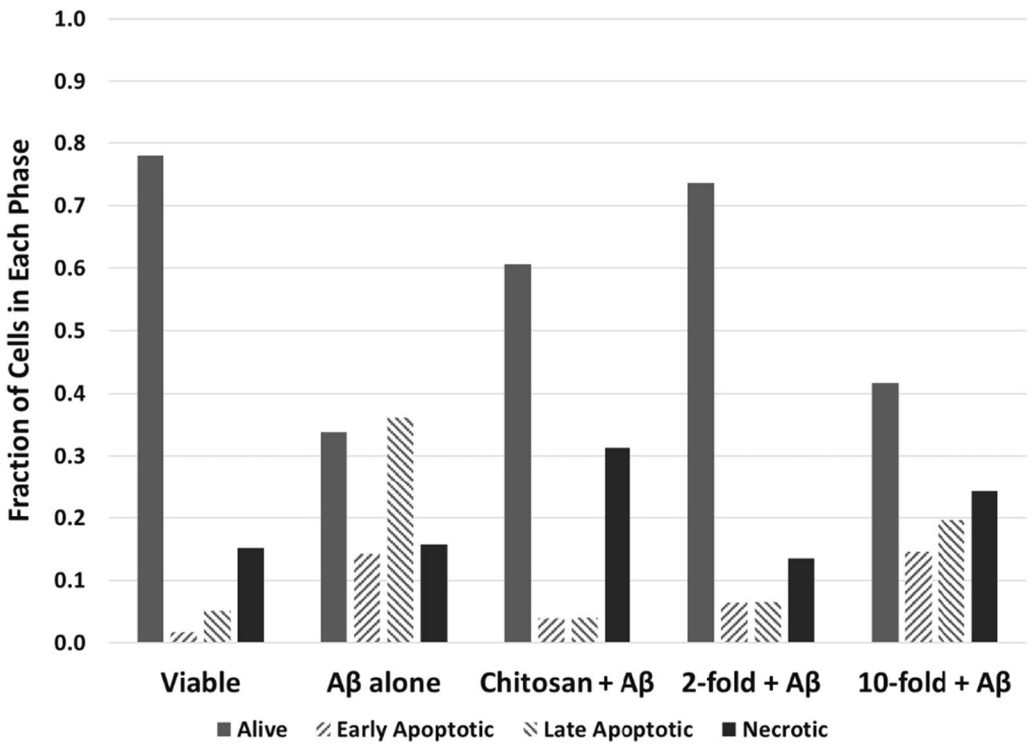

Fig. 7 Protective properties of chitosan and chitosan/SA compounds as measure by FCMS. Each grouping represents a cell treatment, while the different bars represent phase of cell viability for each sample of cells

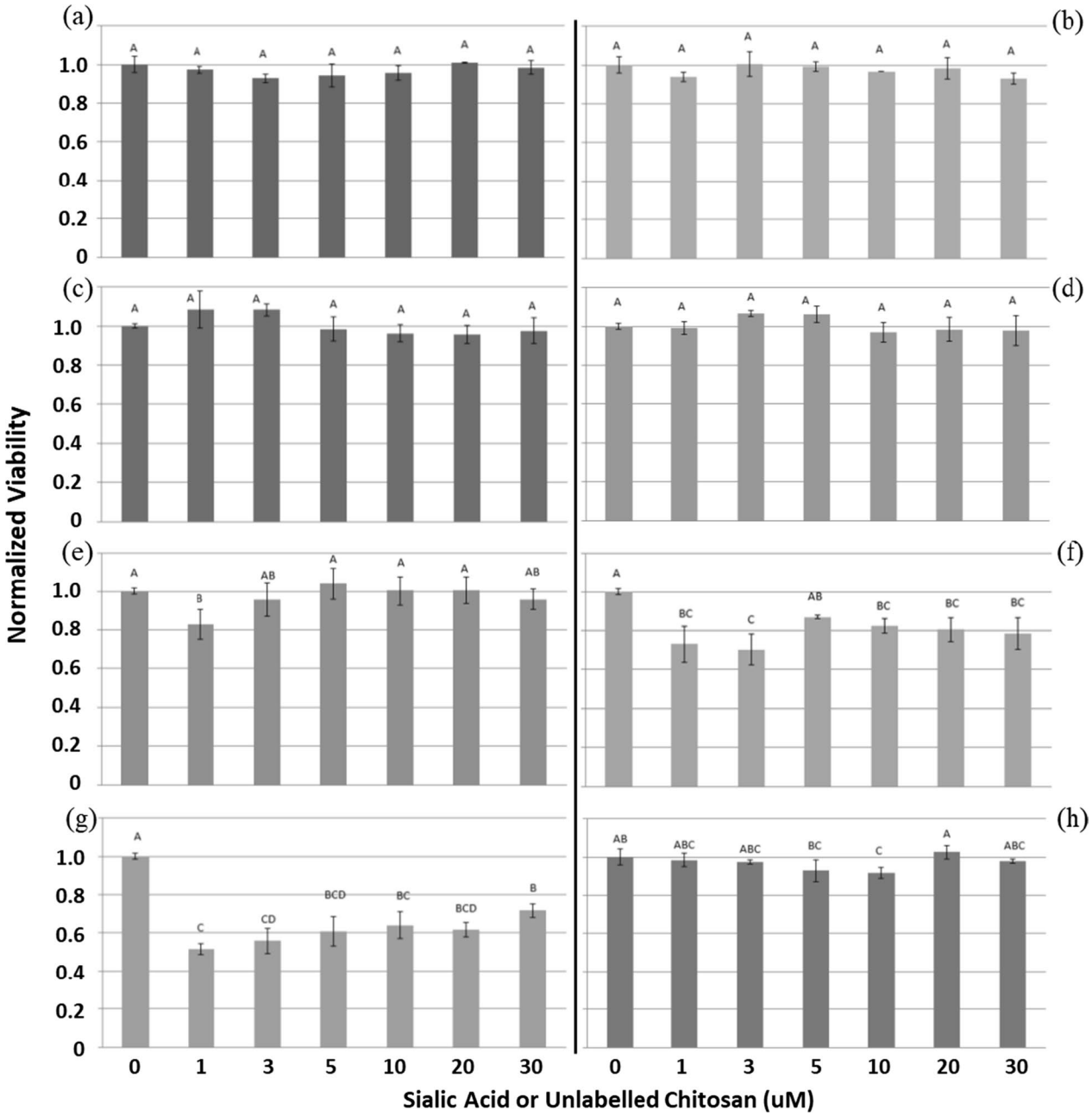

Fig. 8 Statistical analysis of intrinsic toxicity using Tukey analysis for **a** Complex A, **b** Complex B, **c** Complex C, **d** Complex D, **e** Complex E, **f** Complex F, (**g**) Complex G, and **h** Unlabeled chitosan. Any bars labeled with the same letter within a given panel show no statistical difference in normalized viabilities as given by Tukey's test at $p < 0.05$. Each panel should be considered separately when comparing lettering. The panels are grouped to maintain continuity with similar content and analysis. Error bars represent standard error in the data

For all sample sets, there was strong statistical evidence of Aβ toxicity attenuation that saturated a levels of 3uM of complex or lower. With maximum protection occurring for complexes C, D, and E. The protection seemed to fall off as sialic acid labeling degree deviated from the middle values.

Figure 12 shows a comparison of toxicity attenuation for all complexes at each concentration of 5uM or less.

Figure 13 shows a comparison all complexes at each concentration 10uM or greater, with the control (no compound introduced) included for comparison.

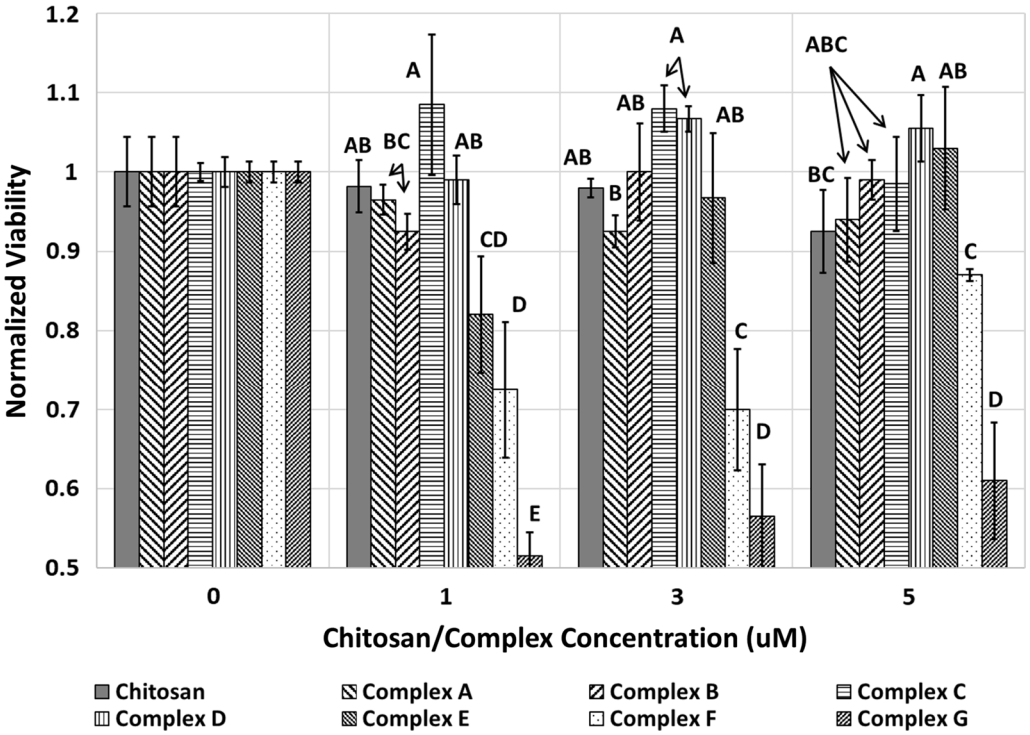

Fig. 9 Statistical analysis of intrinsic toxicity using Tukey analysis across all complexes at low concentrations. Any bars labeled with the same letter within a given concentration grouping show no statistical difference in normalized viabilities as given by Tukey's test at $p < 0.05$. Each concentration grouping should be considered separately when comparing lettering. Error bars represent standard error in the data

Both low and high concentrations of attenuators showed statistically relevant levels of protection, with C, D, and E showing the most beneficial response, on average across all concentrations. As the degrees of labeling deviated from these central values (higher or lower), the protect properties show some minimal waning, while still maintaining a significant degree of attenuation.

Discussion

Sialic acid conjugation

As indicated by the results, the degree of labeling of chitosan with sialic acid shows a concentration dependence during conjugation. This was expected, as the reaction is concentration dependent. However, as there are a limited number of attachment sites on chitosan, the chemistry showed a saturation behavior. While utilizing a chitosan backbone with higher acylation percentage might improve the degree of labeling, it is likely to decrease the flexibility of the final structure, resulting in lower protective properties. Additionally, as indicated in this work, additional sialic acids on the backbone are likely to result in higher toxicity creating an additional negative impact on the compound effectiveness. It is likely that the optimum degree of labeling is, as indicated in this study, between 24.4% and 37.3%, with additional studies being necessary to pinpoint the optimum value more accurately. However, based on the lack of a statistically relevant peak when comparing the central labeling values, the optimum value is likely not to produce statistical different results from the compounds tested in this study.

Efficacy of compounds to prevent toxicity

As shown in Fig. 5, there is a substantial rise in toxicity between the '2 Fold' and '4 Fold' compounds, with minimal toxicity below 2 Fold. This is consistent with the transition to saturation observed in the labeling study, which suggests a correlation between the toxicity and adaptability of the molecule. Additionally, there appears to be an affect with the 10 Fold labeling compound that indicates a decrease in toxicity at higher concentrations. However, shown in the statistical analysis, this increase is not a statistically significant trend, indicating that the 10 Fold compound is actually just inherently toxic and reaching a saturation point of toxicity relatively quickly. This saturation could be related to charge shielding between molecules or media interaction quenching other toxic effects. Additional studies will be necessary to elucidate any potential behavior.

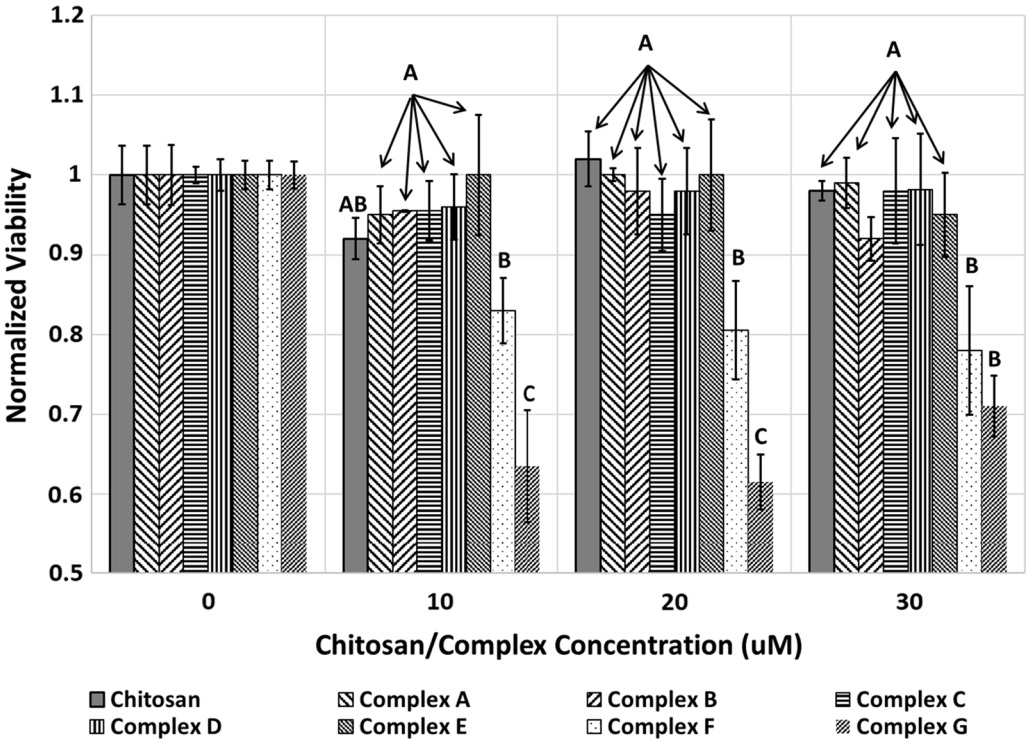

Fig. 10 Statistical analysis of intrinsic toxicity using Tukey analysis across all complexes at high concentrations. Any bars labeled with the same letter within a given concentration grouping show no statistical difference in normalized viabilities as given by Tukey's test at $p < 0.05$. Each concentration grouping should be considered separately when comparing lettering. Error bars represent standard error in the data

As far as protective properties are concerned, Fig. 6 and the statistical analysis around Aβ toxicity attenuation show that for all compounds, there is a statistically significant increase in protection while rapidly reaching the protective maximum (saturation), similar to the saturation effect seen in toxicity. This is potentially due to interactions with cell surfaces creating a bottleneck for protection (as opposed to an interaction with Aβ being the protective mechanism). This possible explanation would account for saturation behaviors, as the cellular decorating could be achieved with lower concentrations that those for Aβ interaction, potentially. This would also be in alignment with results from previous studies with large polymers resulting in similar cellular toxicity saturation (Patel et al. 2007, 2006).

While all compounds (including chitosan) exhibited protective qualities, there was a clear distinction between '2 Fold' and '4 Fold'. This suggests that a compromise can be struck between the degree of sialyation and backbone flexibility (which is crucial for the sialic acid's ability to 'cluster'). Figure 5 also illustrates this change. Even more intriguing is chitosan's ability to demonstrate protective characteristics comparable to sialic acid. The chitosan protective properties are potentially the result of charge surface interactions with the cell blocking Aβ access to the cell (basically, an inverse of the competition reaction seen with sialic acid). While this has promise as a potential protection, there are hazards associated with overloading the cell membrane surface with large polymers, including starvation, ion channel disruption, and agonistic and antagonistic receptor interactions. However, this does suggest that sugar structures may play a crucial role in Aβ binding, suggesting that different biological sugars may be more advantageous than sialic acid.

Apoptosis assay

From the results in Table 3, it appears that the route of cell death (apoptosis vs necrosis) is dependent upon the treatment. As expected, Aβ induced a high level of apoptosis vs necrosis. This was mitigated by the introduction of chitosan and the twofold SA labeled chitosan. However, chitosan appears to induce a twice the level of necrosis to that of Aβ alone, which was not see in the twofold sample. However, the tenfold sample appears to induce a significant amount of cell-death in both mechanisms. These results indicate that the method of protection for the compounds involved may be different. This is further supported by the likely change in compound surface charge upon SA labeling (chitosan showing a positive charge at biological pH with the primary amines and

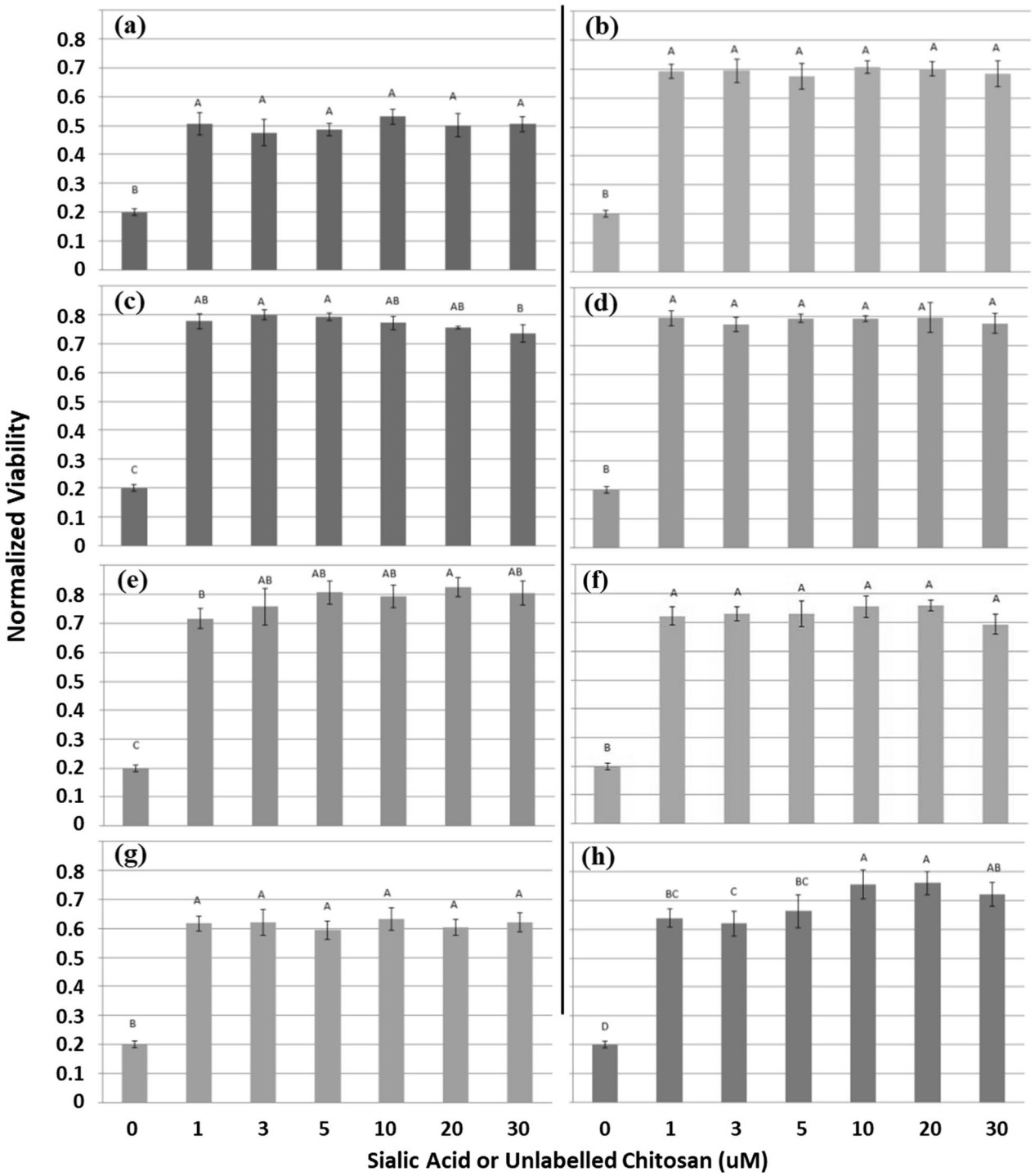

Fig. 11 Statistical analysis of Aβ (50 µM) toxicity attenuation using Tukey analysis for **a** Complex A, **b** Complex B, **c** Complex C, **d** Complex D, **e** Complex E, **f** Complex F, **g** Complex G, and **h** Unlabeled chitosan. Any bars labeled with the same letter within a given panel show no statistical difference in normalized viabilities as given by Tukey's test at $p < 0.05$. Each panel should be considered separately when comparing lettering. The panels are grouped to maintain continuity with similar content and analysis. Error bars represent standard error in the data

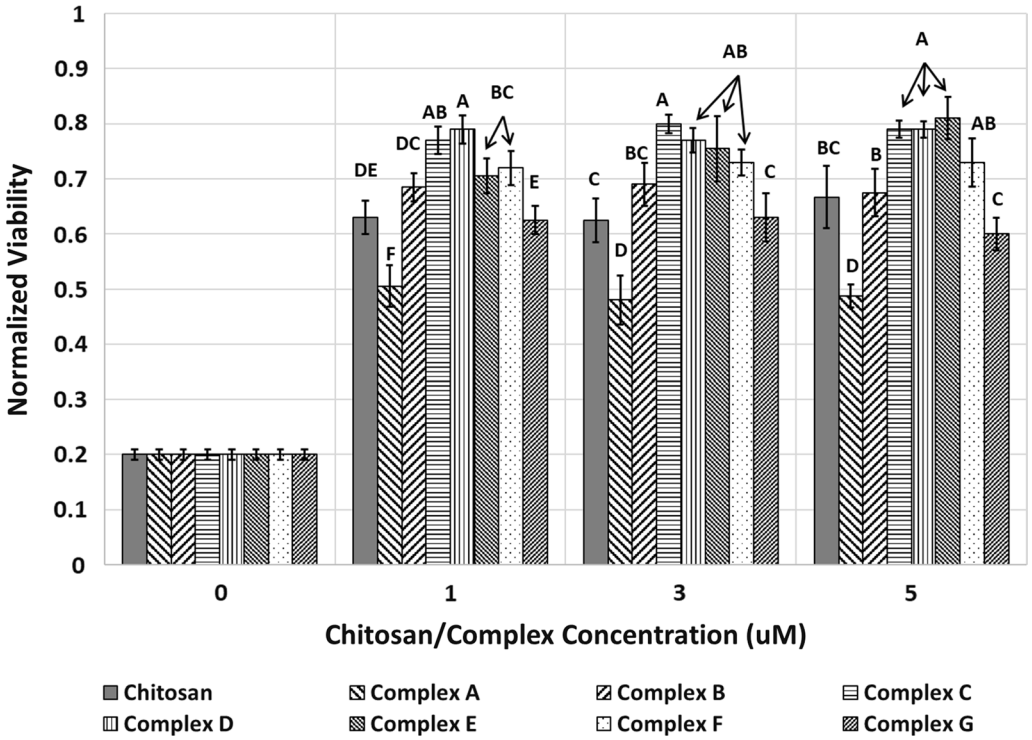

Fig. 12 Statistical analysis of Aβ (50 μM) toxicity attenuation using Tukey analysis across all complexes at low concentrations. Any bars labeled with the same letter within a given concentration grouping show no statistical difference in normalized viabilities as given by Tukey's test at $p < 0.05$. Each concentration grouping should be considered separately when comparing lettering. Error bars represent standard error in the data

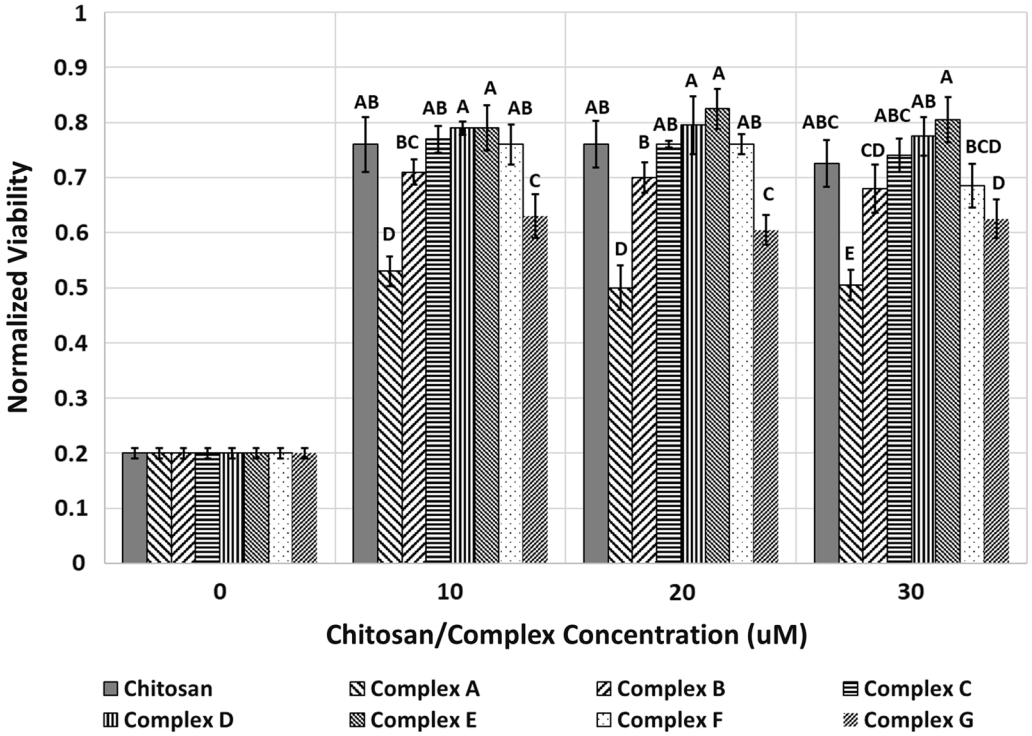

Fig. 13 Statistical analysis of Aβ (50 μM) toxicity attenuation using Tukey analysis across all complexes at low concentrations. Any bars labeled with the same letter within a given concentration grouping show no statistical difference in normalized viabilities as given by Tukey's test at $p < 0.05$. Each concentration grouping should be considered separately when comparing lettering. Error bars represent standard error in the data

SA having a negative charge while reacting to the amines to eliminate their effect). The charge shielding behavior becomes more prevalent at the higher SA labeling.

Conclusions

In this study, the efficiency of chitosan and chitosan/SA compounds in preventing Aβ toxicity is convincingly proven. The narrow error bars in the obtained data demonstrate that the labeling methods produced predictable and reproducible outcomes. In conjunction with the 'peak' protective features of the twofold labeling compound, the saturations behavior of labeling shows a compromise between backbone flexibility and SA clustering effects. Nevertheless, the inherent protective characteristics of chitosan suggest a potential amine-interaction mechanism related with protection. This may be due to charge shielding on the cell surface, which interferes with Aβ binding. Additional testing of chitosan and chitosan analogues should assist in elucidating the mechanism.

Abbreviations

7-AAD	7-Aminoactinomycin D
AB	Amyloid beta peptide
AD	Alzheimer's disease
ATCC	American type culture collection
ATR	Attenuated total reflectance
DI	Deionized
DMSO	Dimethyl sulfoxide
EDC	1-Ethyl-3-(3-dimethylaminopropyl) carbodiimide hydrochloride
FCMS	Flow cytometry and sorting
FTIR	Fourier transform infrared spectroscopy
MES	2-[Morpholino] ethanesulfonic acid
MTT	(3-[4,5-Dimethylthiazol-2-yl)-2,5-diphenyl tetrazolium bromide
NGFß	Human recombinant nerve growth factor beta
NMWL	Nominal molecular weight limit
PBS	Phosphate buffered saline
PE	Phycoerythrin
SA	Sialic acid (N-acetylneuraminic acid)
SH-SY5Y	Human derived neuroblastoma cell line
Sulfo-NHS	N-hydroxysuccinimide

Acknowledgements

The authors want to acknowledge undergraduates Kelsey Tran and Rose Alincastre for their efforts in helping with this work.

Author contributions

DD performed the chitosan conjugation and initial toxicity studies, HKL added in the FCMS related studies and protocol development. PW was integral and data analysis and interpretation of results. JEH was the primary investigator and added all aspects of the project. All authors approved the final manuscript.

Funding

The author received an equipment grant from the National Science Foundation (Grant number MRI-1919295) for the flow cytometry equipment that was utilized in this work. The funding body played no role in the design, collection, analysis, or interpretation of the data. Additionally, the funding agency played no role in writing this manuscript.

Availability of data and materials

All data generated or analyzed during this study are included in this published article.

Declarations

Ethics approval and consent to participate

Not Applicable.

Consent to publication

Not Applicable.

Competing interest

The authors declare that they have no competing interests.

Received: 15 September 2022 Accepted: 29 January 2023
Published online: 09 February 2023

References

Ariga T, Kobayashi K, Hasegawa A, Kiso M, Ishida H, Miyatake T (2001) Characterization of high-affinity binding between gangliosides and amyloid beta-protein. Archiv Biochem Piophys 388(12):225–230. https://doi.org/10.1006/abbi.2001.2304

Alzheimer's association. (2022). Alzheimer's facts and figures report. Retrieved Mar 16, 2022, from https://www.alz.org/alzheimers-dementia/facts-figures

Azmana M, Mahmood S, Hilles AR, Rahman A, Arifin MA, Bin, & Ahmed, S. (2021) A review on chitosan and chitosan-based bionanocomposites: promising material for combatting global issues and its applications. Int J Biol Macromol 185:832–848. https://doi.org/10.1016/J.IJBIOMAC.2021.07.023

Chaudhary PM, Toraskar S, Yadav R, Hande A, Yellin RA, Kikkeri R (2019) Multivalent sialosides: a tool to explore the role of sialic acids in biological processes. Chem Asian J 14(9):1344–1355. https://doi.org/10.1002/ASIA.201900031

Cheeseman J, Kuhnle G, Spencer DIR, Osborn HMI (2021) Assays for the identification and quantification of sialic acids: challenges, opportunities and future perspectives. Bioorganic Med Chem 30:115882. https://doi.org/10.1016/J.BMC.2020.115882

Choo-Smith LPI, Surewicz WK (1997) The interaction between Alzheimer amyloid β(1–40) peptide and ganglioside GM1-containing membranes. FEBS Lett 402(2–3):95–98. https://doi.org/10.1016/S0014-5793(96)01504-9

Cowan C, Patel D, Biology TG-JU (2009) Exploring the mechanism of β-amyloid toxicity attenuation by multivalent sialic acid polymers through the use of mathematical models. J Theor Biol 258(2):189–197. https://doi.org/10.1016/j.jtbi.2009.02.003

Evangelisti E, Cascella R, Becatti M, Marrazza G, Dobson CM, Chiti F, Cecchi C (2016) Binding affinity of amyloid oligomers to cellular membranes is a generic indicator of cellular dysfunction in protein misfolding diseases. Sci Reports. https://doi.org/10.1038/SREP32721

Fantini J, Chahinian H, Yahi N (2020) Progress toward Alzheimer's disease treatment: leveraging the Achilles' heel of Aβ oligomers? Protein Sci 29(8):1748–1759. https://doi.org/10.1002/PRO.3906

Gupta J, Fatima MT, Islam Z, Khan RH, Uversky VN, Salahuddin P (2019) Nanoparticle formulations in the diagnosis and therapy of Alzheimer's disease. Int J Biol Macromol 130:515–526. https://doi.org/10.1016/J.IJBIOMAC.2019.02.156

Kakio A, Nishimoto S, Y K and biophysical research, & 2003, U. (2003). Formation of a membrane-active form of amyloid β-protein in raft-like model membranes. Biochem Biophys Res Commun 303(2): 514–518. https://doi.org/10.1016/S0006-291X(03)00386-3

Lünemann JD, von Gunten S, Neumann H (2021) Targeting sialylation to treat central nervous system diseases. Trends Pharmacol Sci 42(12):998–1008. https://doi.org/10.1016/J.TIPS.2021.09.002

Matsuzaki K (2020) Aβ–ganglioside interactions in the pathogenesis of Alzheimer's disease. Biochimica et Biophysica Acta (BBA) - Biomembranes 1862(8): 183233. https://doi.org/10.1016/J.BBAMEM.2020.183233

Murray HC, Low VF, Swanson MEV, Dieriks BV, Turner C, Faull RLM, Curtis MA (2016) Distribution of PSA-NCAM in normal, Alzheimer's and Parkinson's

disease human brain. Neuroscience 330:359–375. https://doi.org/10.1016/J.NEUROSCIENCE.2016.06.003
Negm NA, Hefni HHH, Abd-Elaal AAA, Badr EA, Abou Kana MTH (2020) Advancement on modification of chitosan biopolymer and its potential applications. Int J Biol Macromol 152:681–702. https://doi.org/10.1016/J.IJBIOMAC.2020.02.196
Patel D, Henry J, & Good T (2006) Attenuation of *β*-amyloid induced toxicity by sialic acid-conjugated dendrimeric polymers. Biochimica et Biophysica Acta (BBA) - General Subjects 1760(12): 1802–1809. https://doi.org/10.1016/J.BBAGEN.2006.08.008
Patel DA, Henry JE, Good TA (2007) Attenuation of β-amyloid-induced toxicity by sialic-acid-conjugated dendrimers: role of sialic acid attachment. Brain Res 1161(1):95–105. https://doi.org/10.1016/J.BRAINRES.2007.05.055
Rawal P, Zhao L (2021) Sialometabolism in brain health and Alzheimer's disease. Front Neurosci 15:308. https://doi.org/10.3389/FNINS.2021.648617/BIBTEX
Rudajev V, Novotny J (2020) The role of lipid environment in ganglioside GM1-induced amyloid β aggregation. Membranes 10(9):1–22. https://doi.org/10.3390/MEMBRANES10090226
Rymer D, Good T (2001) The role of G protein activation in the toxicity of amyloidogenic Aβ-(1–40) Aβ-(25–35) and bovine calcitonin. J Biol Chem 276(4):P2523-2530. https://doi.org/10.1074/jbc.M005800200
Schmidt M, Sachse C, Richter W, Xu C, Fändrich M, Grigorieff N (2009) Comparison of Alzheimer Aβ(1–40) and Aβ(1–42) amyloid fibrils reveals similar protofilament structures. Proc Natl Acad Sci USA 106(47):19813–19818. https://doi.org/10.1073/PNAS.0905007106/SUPPL_FILE/0905007106SI.PDF
Sgambati E, Tani A, Leri M, Delfino G, Zecchi-Orlandini S, Bucciantini M, Nosi D (2022) Correlation between sialylation status and cell susceptibility to amyloid toxicity. Cells. https://doi.org/10.3390/CELLS11040601
Shin MK, Choi MS, Chae HJ, Kim JW, Kim HG, Kim KL (2019) (2019) Ganglioside GQ1b ameliorates cognitive impairments in an Alzheimer's disease mouse model, and causes reduction of amyloid precursor protein. Sci Reports 9(1):1–11. https://doi.org/10.1038/s41598-019-44739-6
Wakabayashi M, Okada T, Kozutsumi Y, Matsuzaki K (2005) GM1 ganglioside-mediated accumulation of amyloid *β*-protein on cell membranes. Biochem Biophys Res Commun 328(4):1019–1023. https://doi.org/10.1016/j.bbrc.2005.01.060
Wang W, Xue C, Mao X (2020b) Chitosan: structural modification, biological activity and application. Int J Biol Macromol 164:4532–4546. https://doi.org/10.1016/J.IJBIOMAC.2020.09.042
Wang W, Meng Q, Li Q, Liu J, Zhou M, Jin Z, Zhao K (2020a) Chitosan derivatives and their application in biomedicine. Int J Molecul Sci. https://doi.org/10.3390/IJMS21020487
Warren L (1963) [67] Thiobarbituric acid assay of sialic acids. Methods Enzymol 6(C):463–465. https://doi.org/10.1016/0076-6879(63)06207-8
Wu J, Wu M, Zhang H, Zhan X, Wu N (2021) An oligomannuronic acid-sialic acid conjugate capable of inhibiting Aβ42 Aggregation and alleviating the inflammatory response of BV-2 microglia. Int J Molecul Sci 22(22):12338. https://doi.org/10.3390/IJMS222212338
Zaman M, Khan MV, Zakariya SM, Nusrat S, Meeran SM, Alam P, Khan RH (2018) Amino group of salicylic acid exhibits enhanced inhibitory potential against insulin amyloid fibrillation with protective aptitude toward amyloid induced cytotoxicity. J Cell Biochem 119(5):3945–3956. https://doi.org/10.1002/JCB.26538

Publisher's Note